

# Integrating Remote Sensing and GIS for Groundwater Potential Mapping in the Santa-Babadjou Corridor

Besende D. Njumba<sup>1\*</sup>, Mary Lum Fonteh Niba<sup>2</sup>, Jane Francis Banseka Ndefru<sup>1</sup>

<sup>1</sup>Department of Geography and Planning, The University of Bamenda, Bamenda, Cameroon

<sup>2</sup>Department of Geography, Higher Teachers Training College Bambili, University of Bamenda, Bamenda, Cameroon

Email: \*besnju@gmail.com, mariefontehriba3@gmail.com and jbanseka@yahoo.com

**How to cite this paper:** Njumba, B. D., Niba, M. L. F., & Ndefru, J. B. (2025). Integrating Remote Sensing and GIS for Groundwater Potential Mapping in the Santa-Babadjou Corridor. *Journal of Geoscience and Environment Protection*, 13, 1-26.

<https://doi.org/10.4236/gep.2025.138001>

**Received:** June 28, 2025

**Accepted:** August 11, 2025

**Published:** August 14, 2025

Copyright © 2025 by author(s) and Scientific Research Publishing Inc.

This work is licensed under the Creative Commons Attribution International License (CC BY 4.0).

<http://creativecommons.org/licenses/by/4.0/>



Open Access

## Abstract

Groundwater scarcity in the Santa-Babadjou Corridor, Cameroon, driven by geological complexity, climate variability, and increasing agricultural demand, necessitates precise identification of potential recharge zones. This study integrates remote sensing (RS), Geographic Information Systems (GIS), and field surveys to delineate groundwater potential zones (GWPZs) using a multi-criteria decision-making approach. Five thematic layers, lithology, slope, relief, drainage density, and land use/land cover (LULC) were analyzed and weighted using the Analytic Hierarchy Process (AHP), yielding a consistency ratio of 1.84%, confirming AHP model reliability. Lithology (32.7%) and slope (29.9%) emerged as the most influential factors, with fractured granites and alluvial deposits exhibiting high infiltration capacity, while steep slopes (>19°) hindered recharge. Moderate-to-high potential zones (95.11% of the area) were concentrated in low-lying regions with gentle slopes, permeable lithologies, and favorable LULC, whereas poor zones (4.90%) coincided with rugged, impermeable terrains. Field validation using spring locations confirmed the model's accuracy. The resulting GWPZ map provides a critical tool for sustainable groundwater management, aiding borehole siting, agricultural planning, and policy decisions in this water-stressed region. This study demonstrates the efficacy of RS-GIS-AHP integration in complex hydrogeological settings, offering a replicable framework for similar regions globally.

## Keywords

Groundwater Potential Zones, Remote Sensing, GIS, AHP, Santa-Babadjou Corridor, Sustainable Water Management

## 1. Introduction

In many developing countries, water scarcity isn't just about a lack of natural resources. It's often the result of deeper seated, human-made challenges, that have crystalized into poor management practices, the absence of clear-cut national water management policies, neglected and crumbling water holding and transportation infrastructure, corruption, and limited financial support (Mahindawansha & Gassmann, 2024; Medhi & Choudhury, 2025; Medrano-Pérez et al., 2023; Mohammed et al., 2025; Mu et al., 2025; Ngwese et al., 2025). These challenges play significant roles in making clean, reliable water difficult to access for millions of people (Abdelkareem et al., 2024; Aind et al., 2025). As a result, many communities in these parts of the world have heavily tilted reliance on groundwater as the most dependable alternative source of clean drinking water. In these zones, unplanned development in the form of ever expanding agricultural fields, built-up, climate change, excessive deforestations and pollution of natural springs, access to groundwater is growing towards the extensive utilization of wells and boreholes (Abdelkareem et al., 2024; Adiat et al., 2024; Alarifi et al., 2022; Arauzo et al., 2019; Ashagrie et al., 2025; Aumar et al., 2023; Boas & Mallants, 2022; Deka et al., 2025). However, the availability of groundwater is unevenly distributed across the globe, making access challenging for many regions (Ishola et al., 2023; Kaushik et al., 2023; Ma et al., 2024; Mahindawansha & Gassmann, 2024; Mosaad et al., 2024).

This is particularly evident in the Santa-Babadjou Corridor, located within the Western Highlands of Cameroon. The geological changes in this region have led to significant variability in groundwater availability. Even within short distances, such as between neighboring communities, the groundwater table can vary widely. This often results in dry well/boreholes or deeper water levels in certain areas, making reliable access to groundwater a persistent challenge in the corridor (Mfonka et al., 2025; Momo et al., 2020; Azinwi Tamfuh et al., 2020; Yasmine et al., 2024).

The Santa-Babadjou Corridor is sandwiched in the Northwest and West Regions of Cameroon, serving as a gateway into both regions. Geographically, the corridor lies between latitude 5°42' to 5°54' N and longitude 10°00'E to 10°18'E. The corridor spans two sub-divisional headquarters Santa in the Northwest and Babadjou in the West. The maps in **Figure 1** provide a visual representation of the corridor; Map 1a shows its position within the broader Northwest and West Regions; Map 1b highlights its placement within Mezam and Bamboutos Divisions; and Map 1c offers a detailed view of the corridor's geographic and agricultural features. The corridor is approximately 62 km from Bamenda, with Santa about 23 km away and Babadjou about 39 km. It is bordered by Batibo and Lebialem to the west and southwest, Menoua to the southwest, Bamenda I and II to the north, Bali to the northwest, Mbouda to the south and southeast, Foubot to the east, and Balikumbat in the Ndop Central Subdivision to the northeast. The location of this corridor makes it a highly strategic agricultural hub, which has over time attracted significant population expansion; this expansion has simultaneously negatively affected the surface water resources in the corridor. Faced with these water

scarcity challenge in an active agricultural basin, individuals have increasingly turned to groundwater extraction through boreholes and wells. Despite conducting site-specific geophysical surveys, many boreholes have failed, resulting in numerous dry wells. These frequent failures are largely attributed to the geological complexity of the terrain located within the Cameroon volcanic line. These failures have been compounded by the absence of detailed geological and hydrogeological studies, as well as limited geophysical data. Geophysical surveys yield better results when integrated with a thorough understanding of the area's geological and hydrogeological conditions. Therefore, assessing and zoning groundwater potential, along with proper planning and management of groundwater resources, is essential for sustainable water access in the corridor.

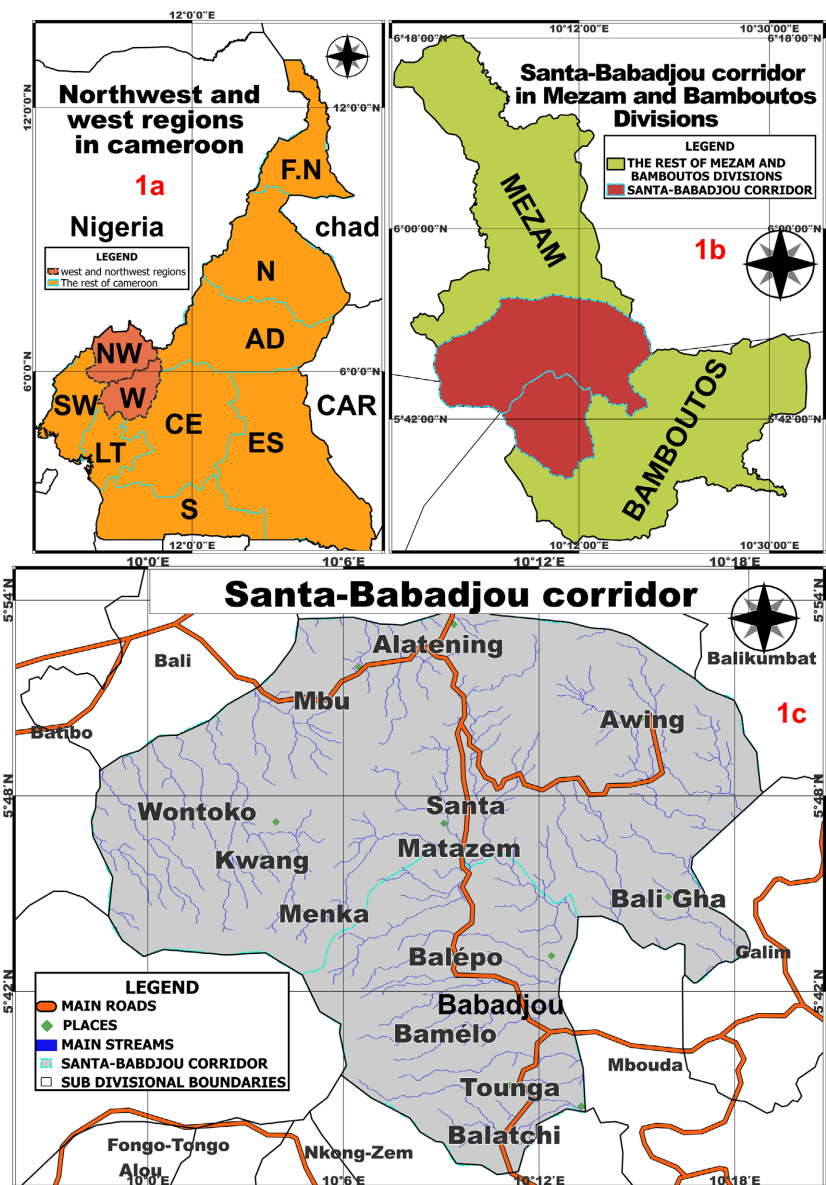


**Figure 1.** Location of Santa-Babadjou Corridor in Mezam and Bamboutos division of Cameroon.

In addition to geophysical surveys, geospatial techniques offer valuable support for groundwater exploration. Mapping (GWPZ) is a crucial step prior to conducting detailed geophysical surveys for effective wells/borehole siting. To assess groundwater potential and improve drilling success, researchers globally have adopted RS and GIS technologies due to their efficiency in terms of time and cost (Abate et al., 2022; Abd-Elmaboud et al., 2024; Abdelouhed et al., 2021; Abdullahi et al., 2023; Abijith et al., 2020; Adesola et al., 2025; Adiat et al., 2024; Agogue Feujio et al., 2024; Ahmad et al., 2020; Ahmed et al., 2025; Akeredolu et al., 2025; Akiang et al., 2025; Alao & Abubakar, 2025; Alikhanov et al., 2021; Arthur et al., 2025; Arunbose et al., 2021; Aulenta et al., 2025; Azinwi Tamfuh et al., 2020). Groundwater potential is influenced by factors that affect recharge, such as relief, land cover and land use, drainage density, vegetation, slope aspect, rainfall, and soil type (Arshad et al., 2020; Arthur et al., 2025; Arunbose et al., 2021; Banerjee et al., 2021). though these vary depending on regional characteristics. These factors are typically analyzed and prioritized using methods like the Multi-Influencing Factor (MIF) technique and the Analytic Hierarchy Process (AHP) to generate accurate groundwater potential maps (Agogue Feujio et al., 2024).

This study integrates remote sensing, geospatial techniques, and field surveys to delineate groundwater potential zones across the Santa-Babadjou Corridor. This approach was based on key factors influencing groundwater recharge in the corridor, including lithology, slope, drainage density, relief, and land use. Each thematic map generated from these factors provides valuable insights into the presence and distribution of groundwater resources. To ensure accuracy, the identified groundwater potential zones were validated using data from existing springs, boreholes, and static groundwater level measurements within the corridor. The findings from this study offer a practical guide for siting new wells/boreholes and will support local farmers, authorities and decision-makers in future planning initiatives, such as zoning new settlements and managing groundwater resources more sustainably.

## 2. Materials and Methods

### 2.1. Location Characteristics of the Santa-Babadjou Corridor

The Santa-Babadjou Corridor, located in the Western and North-Western regions of Cameroon, spans approximately 34 km north to south and 38 km west to east, covering a total area of about 1292 square kilometers. This region is defined by a diverse physical landscape that includes mountains, valleys, forests, springs, crop fields, and clustered farming communities. Its physical environment is shaped by a Guinea-type climate, with annual rainfall ranging between 2000 and 3000 mm and temperatures fluctuating between 15°C and 25°C. These climatic conditions directly influence water availability, crop growth, and overall agricultural activity. The corridor's relief is characterized by scenic hills and plateaux of varying sizes and slopes, with elevations ranging from 1300 meters in Bali-Gham and Awing to 2703 meters near the Wabane boundary. Mt. Lefo in Awing, standing at 2300 me-

ters, is the second-highest peak in the North West Region. Numerous valleys, shaped by the erosive action of flowing streams, enhance drainage and support farming. The drainage system is complex, dominated by the Santa Stream and its numerous tributaries, which create a dense hydrological network crucial for water supply and irrigation. Soil types across the corridor also vary significantly, influencing agricultural potential. Fertile alluvial soils dominate the floodplains and lowlands areas of Maforbe, Matazen, and Kombou, enriched by seasonal sediment deposits. In highland areas such as Akum, Baba, Mbu, and Awing, modified orthic soils offer good drainage, reducing waterlogging. Meanwhile, parts of Santa contain humic or black soils rich in organic matter, which retain moisture effectively. Together, these interconnected climatic, topographic, hydrological, and soil features create a dynamic environment that supports diverse agricultural systems and shapes water resource availability across the Santa-Babadjou Corridor (Achu et al., 2020; Mfonka et al., 2025; Momo et al., 2020; Azinwi Tamfuh et al., 2020; Yasmine et al., 2024).

The methodological framework illustrated in **Figure 2** was systematically followed. Remotely sensed data were utilized to develop a series of thematic layers, which were subsequently integrated to generate the GWPZ map. To ensure the reliability of the GWPZ outputs, field verification and validation as shown in **Table 1** were carried out using a combination of existing spring locations and static groundwater level measurements. In this regard, Field validation was conducted using a total of 33 ground-truth points, consisting of 14 springs, 12 boreholes, and 7 static groundwater level measurement points, spatially distributed across the Santa-Babadjou Corridor. These validation points were overlaid on the final Groundwater Potential Zone (GWPZ) map to assess model accuracy. Results indicate that 28 out of the 33 validation points (equivalent to 84.8%) fall within zones classified as moderate to very high groundwater potential. The various phases of this approach are elaborated in the subsequent sections. Phase (1) involved, the identification and mapping of surface factors that influence groundwater recharge, runoff, occurrence, and storage; Phase (2) involved, the reclassification of each of these factors based on their relative impact on recharge potential; and Phase (3) focused on assigning appropriate weights to each thematic layer to reflect its significance in contributing to groundwater availability. A rank and weight were assigned to each factor based on its relative importance to groundwater recharge. Finally, all thematic maps were integrated in ArcGIS 10.5 using the weighted overlay analysis method to generate the GWPZ map.

In this study, five key factors were considered: lithology, slope, relief, drainage density, and land use. The slope and drainage density maps were derived from Shuttle Radar Topography Mission (SRTM) Digital Elevation Model (DEM) data with a 30-meter spatial resolution (SRTM1N04E009V3) using ArcGIS 10.5. Relief and Land Use thematic layers were generated from Band 7 of Landsat 8 OLI imagery (LC08\_L1TP\_187057\_20170507\_20170515\_01\_T1), which covers the entire Santa-Babadjou Corridor. The slope, drainage, and Relief maps were created us-

ing the Spatial Analyst tools, while the land use map was developed using the supervised maximum likelihood classification tools in ArcGIS 10.5. Lithological data were also incorporated as a crucial factor influencing groundwater movement and storage within the study area.

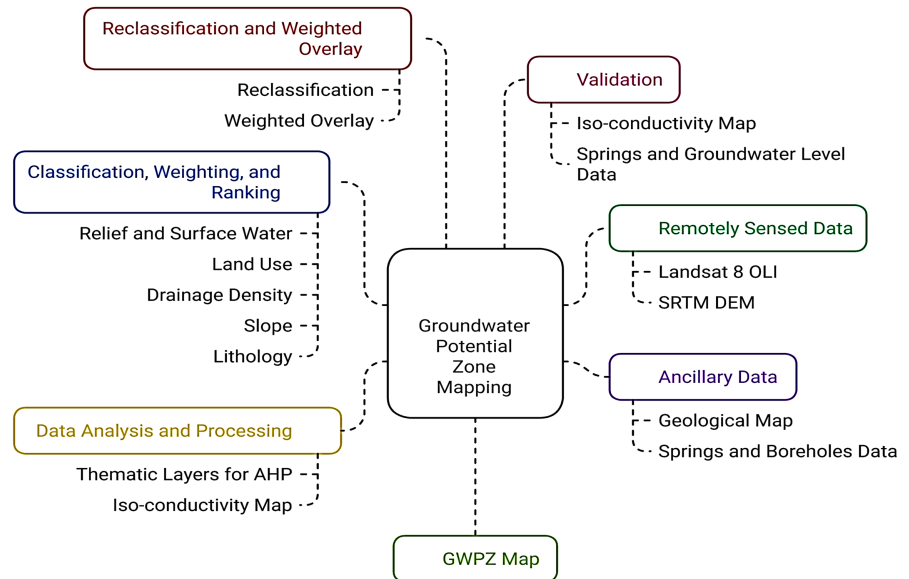


**Figure 2.** Methodological flow chart used for this study.

**Table 1.** Summary of validation results showing the number and percentage of ground-truth points (springs, boreholes, and static water level measurements) groundwater potential zone category in the Santa-Babadjou Corridor.

Groundwater Potential Zone	Number of Validation Points	Percentage of Total (%)
Very High Potential	9	27.3
High Potential	11	33.3
Moderate Potential	8	24.2
Low Potential	4	12.1
Very Low Potential	1	3.1
Total	33	100

The lithology map was reproduced from the Multi-Source Satellite Imagery and Machine Learning for Detecting Geological Formations in Cameroon’s Western Highlands by (Ayikpa et al., 2025).

The five thematic layers of lithology, slope, relief, drainage density, and land use/land cover (LULC) were selected for this study based on their direct influence on groundwater recharge and storage dynamics in the Santa-Babadjou Corridor, as well as the availability of reliable spatial data.

Lithology was prioritized because fractured and porous geological formations

such as Late Tectonic Granites and alluviums significantly influence infiltration and aquifer storage capacity. Slope was included due to its control over surface runoff and infiltration, where gentler slopes promote groundwater recharge, especially in the steep terrains of the corridor. Relief reflects elevation differences that affect surface water accumulation, with low-lying areas enhancing recharge. Drainage density was used to indicate runoff potential; lower densities allow more time for water to percolate into the ground. LULC was considered to assess how different land covers affect infiltration, with farmlands and grasslands promoting recharge while built-up areas hinder it.

While theoretically important for recharge modeling, we faced significant administrative challenges in obtaining reliable, community-level rainfall data from local meteorological authorities due to data-sharing restrictions and sparse monitoring station coverage across the corridor. Given these constraints and the region's relatively uniform annual rainfall distribution (2000 - 3000 mm/yr), we prioritized more readily available and spatially variable factors (lithology, slope) that better discriminate recharge potential at our study scale. Soil texture was excluded because of the low resolution of regional maps and because lithology and slope have greater control over infiltration in volcanic terrains like the corridor. Lineament density was not included because, its effects are partially captured through the lithology and slope layers which indirectly account for structural controls.

This focused selection ensured a parsimonious model while accounting for over 90% of recharge variability, as confirmed by field validation, with a consistency ratio (CR) of 1.84%.

## 2.2. The Analytic Hierarchy Process (AHP)

To minimize errors and maintain the geometric integrity of the imagery, all thematic layers were standardized and projected onto a common Universal Transverse Mercator (UTM) coordinate system (WGS84 Zone 32N) with a spatial resolution of 30 meters. The five thematic maps generated through this process served as key input factors for producing the GWPZ map using the AHP. AHP is a multi-criteria decision-making method developed by Thomas (Saaty, 1984), which involves calculating weights by determining the dominant right eigenvector of a positive reciprocal decision matrix. This matrix is constructed from pairwise comparisons, using a fundamental scale of values to express relative importance. This was achieved using the Analytic Hierarchy Process Software developed by Klaus Goepel (2024), the five criteria (factors) were subjected to pairwise comparisons, as shown on equations 1 and 2 below.

$$pwc = (a_1, a_2, \dots, a_{npc}) / (x_1, x_2, \dots, x_{npc}) \quad (1)$$

Each integer  $a_i$  falls within the range  $[0, 1]$ , while  $x_i$  ranges from  $[1, M]$ , where  $M = 9$  and  $i = 1, 2, \dots, npc$ , with  $npc$  representing the number of pairwise comparisons. For  $n$  criteria, a corresponding  $n \times n$  decision matrix is constructed and populated using the values from the pairwise comparison ( $pwc$ ) vector

(equations 2)

$$npc = (N^2 - N) / 2 \quad (2)$$

The five influencing factors, along with their assigned weights, were geopro-cessed using the Weighted Overlay tool under the Spatial Analyst Tools in ArcGIS 10.5 to produce the GWPZ map. Prior to analysis, all input criteria were reclassified into integer rasters. A scale of 1 to 5 was applied, where 1 denotes the least favorable and 5 the most favorable conditions for groundwater recharge and occurrence. This scale was set through the Evaluation Scale parameter to guide the assignment of relative suitability scores during overlay analysis.

### 3. Results and Interpretation

The results obtained from the analysis of various factors (lithology, land use, relief, drainage density, slope, existing springs, and static water levels) are presented and discussed in the proceeding sections.

#### 3.1. Factors Influencing Groundwater Recharge

##### 3.1.1. Geological Structure of the Santa-Babadjou Corridor

The geological structure of the Santa-Babadjou Corridor plays a fundamental role in determining the potential for groundwater recharge and subsurface water flow. Among all influencing factors, lithology stands out as the most critical in controlling both the occurrence and movement of groundwater in the corridor (**Table 2**). Effective groundwater recharge relies on the presence of suitable geological formations that allow for the infiltration and storage of water in aquifers. As illustrated in **Figure 3**, the corridor is characterized by a diverse assemblage of rock types, each with varying implications for infiltration, porosity, and water retention.

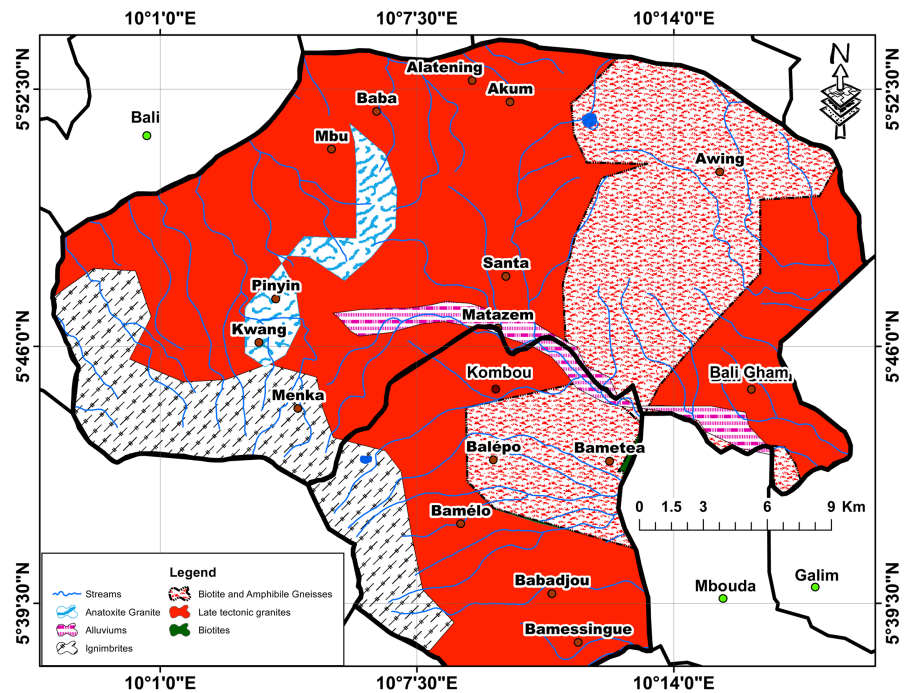
**Table 2.** Class ranking and percentage of thematic weight of each factor used in the Groundwater Potential Zone map.

Factor/criterion	Class/value range	Rating	Reclassified value	Scale/rank	Weight/priority
Lithology	Alluviums	1	1	5	32.7
	Fractured Late Tectonic Granites	2	2	4	
	Ignimbrites	3	3	3	
	Biotite & Amphibole Gneisses	4	4	2	
	Anatoxite Granite	5	5	1	
Slope (°)	0.00001 - 3.8	2	1	5	29.9
	3.81 - 5.2	2	5	5	
	5.21 - 8.9	3	4	4	
	8.91 - 19.0	4	2	2	
	19.1 - 46.0	5	1	1	

Continued

Relief and current surface water	Very low	3	1	3	17.9
	Low	2	3	3	
	Moderate	3	4	4	
	High	4	5	5	
	Very high	5	5	5	
Drainage density (km/km <sup>2</sup> )	Very low	4	1	5	10.4
	Low	2	5	5	
	Moderate	3	4	4	
	High	4	3	3	
	Very high	5	2	2	
Land use	Built-up	5	1	3	6.8
	Forest	2	1	1	
	Grasslands	3	3	3	
	Farmlands	4	4	4	

Source: Generated from AHP-OS.



Source: Redrawn from (Njumba et al., 2023).

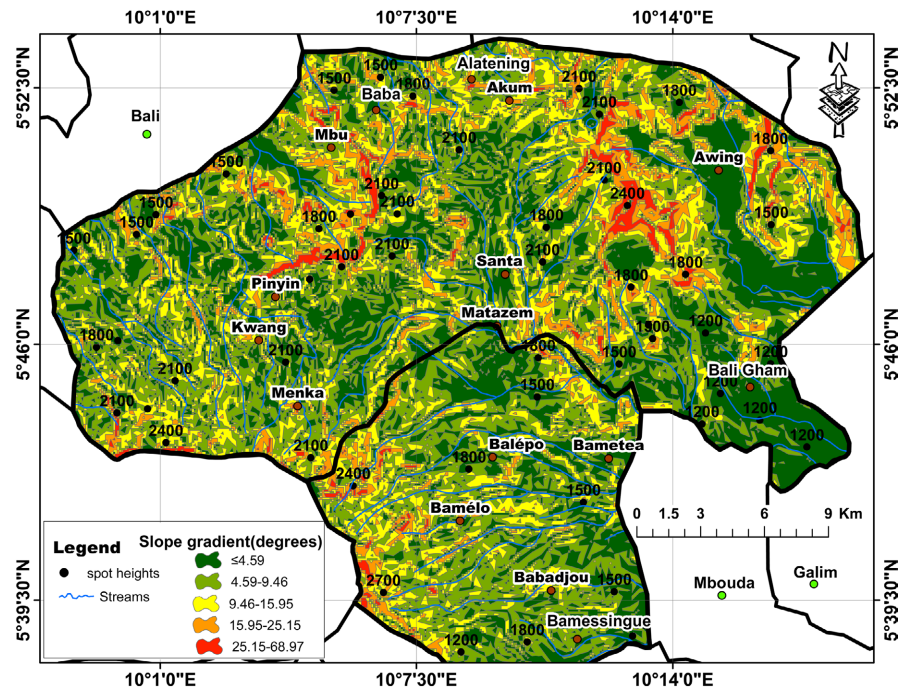
**Figure 3.** Geologic map of the Santa-Babadjou Corridor.

The Late Tectonic Granites dominate the area, covering approximately 29.4% of the corridor. These granitic formations, found predominantly in the

Centre, North, Northwest, and Eastern zones, are generally fractured and moderately permeable, offering fair potential for groundwater recharge through secondary porosity developed in joints and cracks. Biotite and Amphibole Gneisses make up 24.6% of the corridor and are located mainly in the Central and Northeastern parts. These metamorphic rocks typically exhibit low primary porosity, but when highly weathered or fractured, support limited groundwater movement and storage. Ignimbrites, occupying about 21.5%, are concentrated on the western flanks of the corridor, particularly along the slopes of the Bamboutos Mountain. These pyroclastic volcanic rocks often exhibit variable permeability, with their recharge potential heavily dependent on the extent of weathering and fracturing. In more fractured zones, they form effective aquifers. Anatoxite Granite, covers approximately 15.3% of the area and distributed across the Northern and Northeastern sectors, also contributes to groundwater dynamics. Though generally less permeable due to its crystalline structure, localized fracturing can enhance infiltration in some parts. Alluviums account for 9.2% of the corridor and are mainly concentrated along wetland zones and stream channels in the Southern and Southwestern parts. These unconsolidated sediments possess high porosity and permeability, making them the most effective geological medium for groundwater recharge in the corridor. The heterogeneity of these geological formations results in spatial variation in groundwater recharge potential across the Santa-Babadjou Corridor. Hence, regions underlain by alluvium and fractured granitic rocks are more favorable for recharge, while areas dominated by unfractured crystalline and metamorphic rocks show relatively lower infiltration capacity. Understanding this geological framework is crucial for guiding water resource management and planning within the corridor.

### 3.1.2. Slope

The Slope of the corridor also plays a crucial role in groundwater recharge potential, as it influences both surface water infiltration and the velocity of runoff. As illustrated in **Table 2**, slope ranks as the second most influential factor in determining recharge potential, with a calculated weight of 29.9. The slope map of the corridor, in **Figure 4**, reveals considerable variations in terrain, ranging from flat low laying regions to steep mountainous areas. The slope across the region is classified into five gradient categories consistent with those used in **Table 3**. These classes were reclassified to reflect their recharge potential, with very gentle and gentle slopes being most favourable due to longer residence time and higher infiltration capacity, while very steep slopes encourage rapid runoff and minimal infiltration. According to **Table 3**, areas with low slopes gradients cover 19.20 ha, very low slopes cover 16.33 ha, moderate slopes 10.93 ha, high slopes 3.79 ha, and very high slopes 0.50 ha, indicating that over half of the corridor consists of slopes below 9°, which are conducive for groundwater recharge.



Source: Estimated from NASA Digital elevation model.

**Figure 4.** Slope variations in the Santa-Babadjou Corridor.

**Table 3.** Slope classification and area distribution in the Santa-Babadjou Corridor.

Slope Class	Slope Range (°)	Slope Category	Area (Ha)	Interpretation (Infiltration Potential)
Very Gentle	0.00 - 3.73	Very Low	16.33	Very High (Favourable for recharge)
Gentle	3.74 - 5.11	Low	19.20	High (Favourable for recharge)
Moderate	5.12 - 8.84	Moderate	10.93	Moderate (Transition zone)
Steep	8.85 - 18.90	High	3.79	Low (Increased runoff)
Very Steep	19.00 - 45.80	Very High	0.50	Very Low (High runoff, low infiltration)

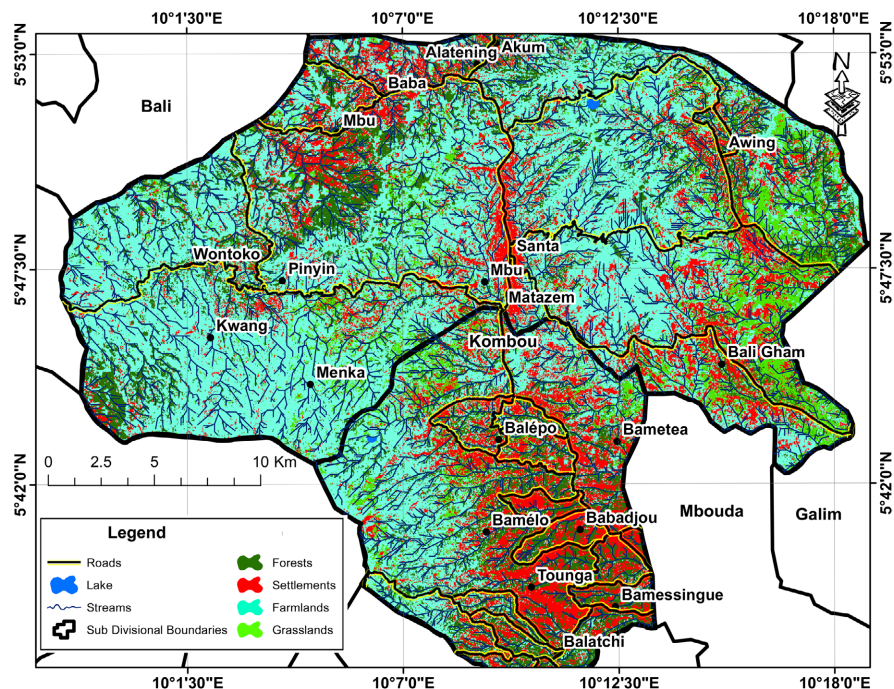
Geographically, the steepest slopes, of  $\geq 19^\circ$ , are concentrated in the Western, Northern, and Northeastern sections of the corridor, particularly in and around Menka, Kwang, Pinyin, Mbu, Alatening, Akum, Awing, and Santa. These regions coincide with the highest elevations in the corridor, like Bamboutos Mountain (up to 2700 m) and Lake Awing (around 2400 m). The steep slopes here, formed primarily through tectonic and geomorphological processes linked to the Cameroon Volcanic Line, result in high surface runoff, minimal infiltration, and increased soil erosion risk, making them less suitable for groundwater recharge.

Moving southwards **Figure 4** illustrates that, the terrain transitions into moderate slopes ( $5.12^\circ - 8.84^\circ$ ) in the central part of the corridor, especially between Matazem, Balepo, and Babadjou, where elevations range between 1500 m and 1800 m. These zones act as intermediaries between steep northern slopes and the gentle southern lowlands. While these moderate slopes still present runoff chal-

lenges, they also offer moderate potential for groundwater recharge if managed properly through runoff mitigation and enhanced infiltration strategies. In contrast, the southern parts of the corridor, including lower-lying areas of Bali Gham, are characterized by gentle to very gentle slopes ( $\leq 9.00^\circ$ ), with elevations ranging from 1200 m to 1500 m. These flatter areas are more favourable for infiltration due to slower runoff, making them ideal for groundwater recharge. Their geomorphology supports water retention and soil stability, reinforcing their role in sustaining surface and subsurface water availability (Abdelouhed et al., 2021; Abdul-lahi et al., 2023; Abdullateef et al., 2021; Achu et al., 2020; Adesola, 2024).

### 3.1.3. Land Use Land Cover of the Santa-Babadjou Corridor

According to the ranking in **Table 2**, LULC represents an important but relatively less influential factor in groundwater recharge potential across the Santa-Babadjou Corridor. Despite contributing the least to groundwater recharge among the evaluated parameters at a calculated weight of 6.8 (**Figure 5**) LULC plays a critical role in regulating water infiltration and storage, (**Figure 5** and **Table 2**) (Adewumi et al., 2023). The dominant land use types identified include farmlands, settlements, forests, grasslands, and water bodies. The analysis reveals that more than 75% of the Santa-Babadjou Corridor is dominated by farmlands and settlements, which profoundly influence surface water dynamics.



Source: Landsat 9 (NASA, 2023).

**Figure 5.** Land use and land cover in the Santa-Babadjou Corridor.

Among these, farmlands, (52%) and grasslands (9%) significantly contribute to enhanced infiltration of surface water into underlying aquifers due to their permeable soil characteristics and reduced surface sealing. On the other hand, built-

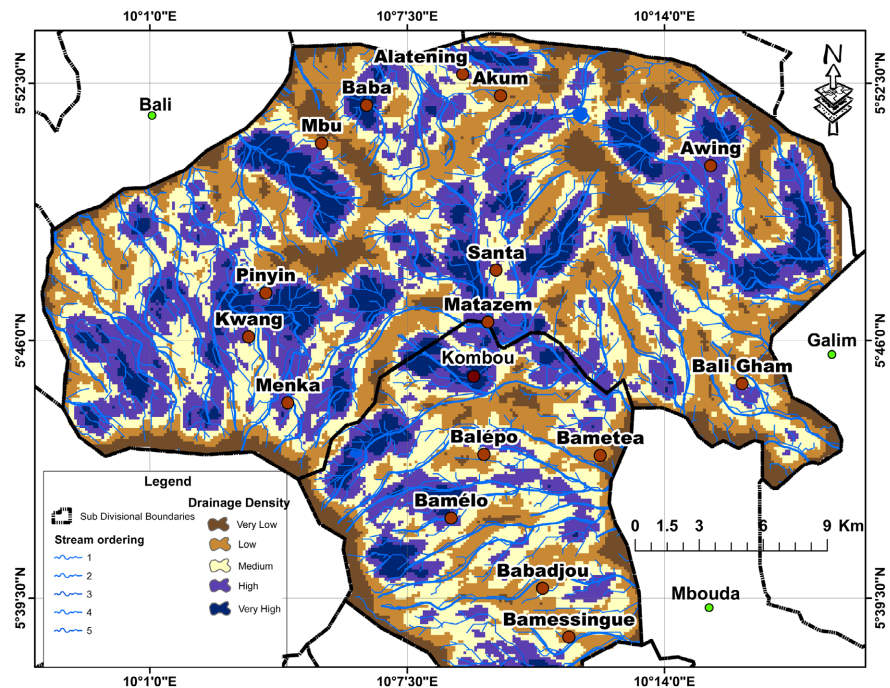
up areas (21%), hosts compact surfaces that hinder infiltration, increase runoff, and reduce recharge potential. These urbanised zones seal the ground, thereby impeding the natural recharge of groundwater systems. Forests, (18%), are typically situated on steep slopes with dense canopies, limiting direct surface water infiltration due to rapid runoff and interception. Meanwhile, water bodies represent a negligible 0.50%, having limited influence on regional recharge but playing a role in water storage and ecosystem support. The Changes in land use patterns especially agricultural expansion and urban development disrupts natural hydrological processes, leading to decreased groundwater recharge, increased pollution loads, and modified surface water flow regimes. For instance, land degradation and deforestation in some parts of the corridor introduce bare surfaces that accelerate runoff and erosion, contributing to sedimentation in water bodies and reduction in infiltration.

#### 3.1.4. Drainage Density

Drainage density is the fourth most influential factors affecting groundwater recharge in the Santa-Babadjou Corridor, with a calculated weight of 10.4% (Table 2). The drainage density of the corridor, as illustrated in Figure 6 and Table 4, highlights the spatial distribution and intensity of stream channels across the landscape. This metric quantifies the total length of stream channels per unit area and plays a critical role in determining the efficiency of surface water transport and runoff within a watershed. High drainage density is generally associated with rapid surface water movement, which reduces the time available for infiltration and increases runoff. According to the classification by Bhadra and Pattanayak (2025), drainage density serves as an indicator of a region's infiltration potential. In the case of the Santa-Babadjou Corridor, a drainage density weight of 10.4% suggests a moderate drainage density, which facilitates a balance between surface runoff and rainfall infiltration into the subsurface. This, in turn, can enhance groundwater recharge and overall water availability. The spatial pattern of drainage in the corridor reflects this balance, making drainage density a key determinant in the hydrological dynamics and water resource management of the region.

The drainage density results in Table 4 illustrate that the Santa-Babadjou Corridor exhibits significant spatial variation, reflecting the diversity in topography, hydrology, and land use across the region. The drainage density patterns in Figure 6 and Table 4 are classified into five categories: very low, low, medium, high, and very high drainage densities. High and Very High Drainage Density zones, covering approximately 556.4 km<sup>2</sup> (43.1%), are mainly concentrated in the low-lying parts of the corridor where gentle gradients and expansive terrain promote the formation of dense stream networks. Medium Drainage Density areas, comprising 322.1 km<sup>2</sup> (24.9%), are found across transitional zones of Bamelo, Bametea, and parts of central Santa. These regions exhibit moderate relief, which allows for a balance between surface runoff and infiltration. The hydrological implications in these zones suggest moderate runoff and infiltration capacity, making them well-suited for aquifer recharge initiatives and rainwater harvesting systems. Low

and Very Low Drainage Density zones, accounting for 413.5 km<sup>2</sup> (32.0%), are predominantly found in the upland and mountainous areas of Kombou, Matazem, Santa, Awing, Pinyin, and Bali Gham. These locations are characterized by steep gradients and rugged terrain, which result in fewer stream networks and enhanced water infiltration into the subsurface.



Source: Estimated from NASA Digital elevation model.

**Figure 6.** Drainage density distribution in the Santa-Babadjou Corridor.

**Table 4.** Drainage density distribution in the Santa-Babadjou Corridor.

Drainage Density Category	Area Coverage (km <sup>2</sup> )	Percentage Coverage (%)
Very Low	168.0	13.0
Low	245.5	19.0
Medium	322.1	24.9
High	356.9	27.6
Very High	199.5	15.5
Total	1292.0	100.0

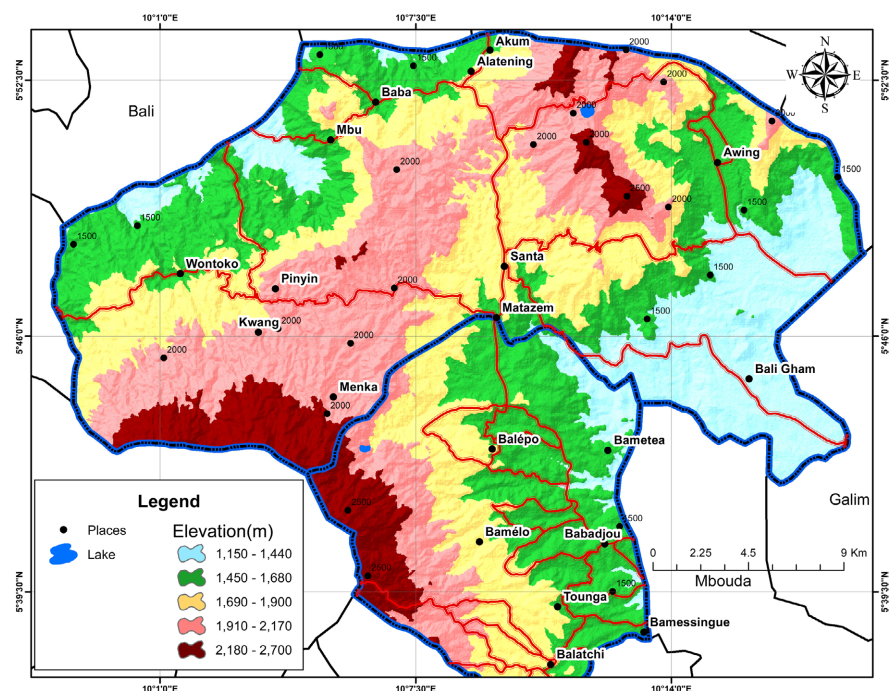
Source: Computed from **Figure 6**.

### 3.1.5. Relief and Current Surface Water

The relief and current surface water of the corridor is ranked third with a calculated weight of 17.9, as shown in **Table 2** hence it plays a significant role in determining groundwater availability. As illustrated in **Figure 7** and **Figure 8**, the relief and current surface water of the corridor reveal a diverse landscape. According to

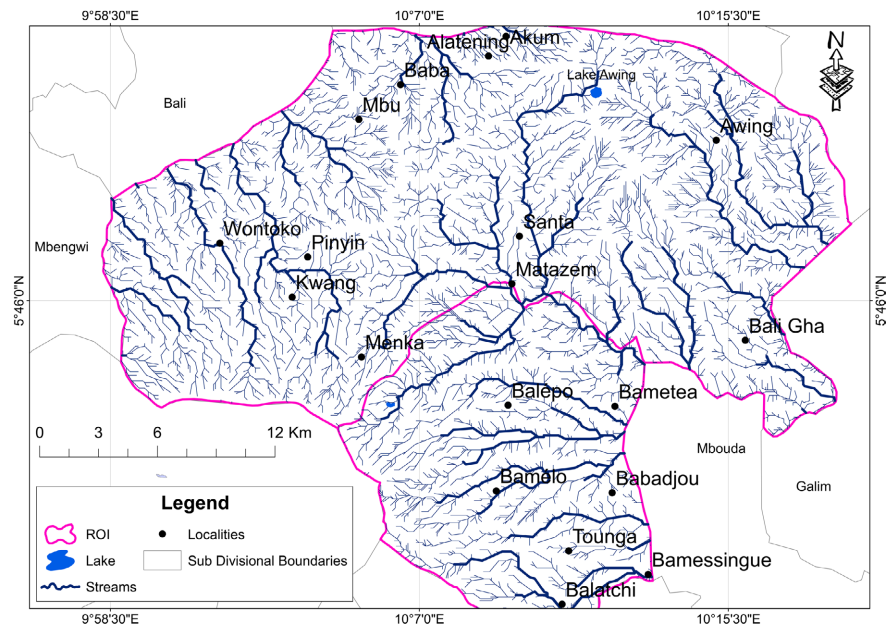
(Ahmadou et al., 2023; Anaba Fotze et al., 2025; Anaba Onana et al., 2017; Are-touyap et al., 2020) the relief and current surface water of the corridor shape the hydrological characteristics of the region. The elevations range from approximately 1300 meters in Bali-Gham and Awing to about 2703 meters at the boundary with Wabane Sub Division. Mount Lefo, located in Awing, stands at 2300 meters, making it the second-highest peak in the North West Region after Mount Oku (Anaba Fotze et al., 2025). The corridor is further intersected by multiple stream valleys, which exert a strong influence on its relief and drainage patterns, as seen in **Figure 8**. These valleys have been carved over time by the erosive forces of upland tributaries, contributing to the complex topography of the area (Ayikpa et al., 2025; Mfonka et al., 2025). The resulting landforms play a vital role in determining water availability and agricultural productivity. From a hydrological perspective, **Figure 7** illustrates how the diverse terrain significantly affects water distribution, flow, and retention. The slopes of hills, whether gentle or steep, influence surface runoff rates and the degree of infiltration into soils.

Steeper areas tend to promote runoff and erosion, reducing water retention, while gentler slopes support better infiltration, enhancing groundwater recharge and soil moisture retention. These processes are vital for maintaining agricultural viability in the corridor. In addition, the river valleys that traverse the Santa-Babadjou Corridor serve as natural drainage channels, redirecting excess rainfall from upland zones and improving water flow throughout the watershed. These valleys are essential for sustaining irrigation systems and enhancing crop production. Their presence not only facilitates drainage and flood management but also improves water accessibility for farming communities across the region.



Source: Geo-Database of Cameroon and NASA Digital elevation model.

**Figure 7.** Relief representation of the Santa-Babadjou Corridor.



Source: Determined from Figure 7.

Figure 8. Occurrence of surface water in the Santa-Babadjou Corridor.

The illustration in Figure 7 and Table 5 reveal that, the Santa-Babadjou Corridor is characterized by significant elevation variability, which directly shapes land use, settlement distribution, agricultural potential, and water resource management. The relief within the corridor ranges from very low elevations of around 1150 meters, found in low-lying valleys zones of Bali Gham and Bametea, to very high mountainous terrains reaching up to approximately 2700 meters in the Bam-boutos Caldera bordering Wabane Subdivision. This variation influences the occurrence of surface water resources (Figure 8) as well as creates distinct ecological zones that influence both natural and human activities.

Table 5. Distribution of relief categories in the Santa-Babadjou Corridor.

Relief Category	Elevation Range (m)	Description	Estimated Area (km <sup>2</sup> )	Coverage (%)
Very Low	1150 - 1440	Valley bottoms, low plains (Bali Gham, Bametea)	181.0	14
Low	1450 - 1680	Lower foothills and undulating areas (Awing, Babadjou, Wontoko)	271.3	21
Medium	1690 - 1900	Moderate plateaux and escarpments (Matazem, Santa)	297.2	23
High	1910 - 2170	Elevated hills and plateaux (Menka, Pinyin, Mbu)	335.9	26
Very High	2180 - 2700	Steep mountain zones and peaks (Lefo, Bali-Gham border)	206.7	16

Source: Computed from Figure 7.

Table 5 reveals that, zones characterized as Very low relief areas, cover about 14% of the corridor (roughly 181.0 km<sup>2</sup>). On the other hand, low relief regions,

which accounts for about 21% (271.3 km<sup>2</sup>), are found in transitional zones of Babadjou. Medium relief zones dominate around Santa and Matazem and constitute approximately 23% (297.2 km<sup>2</sup>) of the corridor. High relief regions, covering 26% of the corridor (about 335.9 km<sup>2</sup>), are mainly located in the southwestern and Northeastern portions, particularly around Pinyin, Mbu, and Menka. These zones are characterized by steep slopes and hilly terrain. These high-relief landscapes are also important for regulating watershed functions, and their forested slopes play a significant role in maintaining the hydrological balance of the region. The very high relief zones, which occupy about 16% (206.7 km<sup>2</sup>), are mostly concentrated along escarpments and mountainous ridges. These areas are characterized by sharp elevation changes and rugged terrain. As a result, they are largely unsuitable for intensive agriculture or dense settlement. However, they are essential for water catchment protection and biodiversity conservation. Their ecological significance cannot be overstated, as they serve as headwaters for many streams in the corridor.

### 3.1.6. Groundwater Potential Zonation Process

As illustrated in **Table 6**, the groundwater potential zonation was achieved using the weighted overlay technique, where five key factors (Lithology, Slope, Relief and current surface water, Drainage density, and Land use) were assigned specific weights and ranks based on their influence on groundwater occurrence. From **Table 5**, the different factors recorded different weights and ranks with Lithology (32.7%, Rank 1), Slope (29.9%, Rank 2), Relief and current surface water (17.9%, Rank 3), Drainage density (10.4%, Rank 4), and Land use (6.8%, Rank 5). The overlay analysis in **Figure 9** and **Table 6** produced five distinct categories of groundwater potential zones, classified as, very poor, poor, moderate, good, and very good. The zones classified as very poor recorded a Consistency Ratio (CR) of 1.84%, indicating an acceptable level of consistency in the multi-criteria decision-making process.

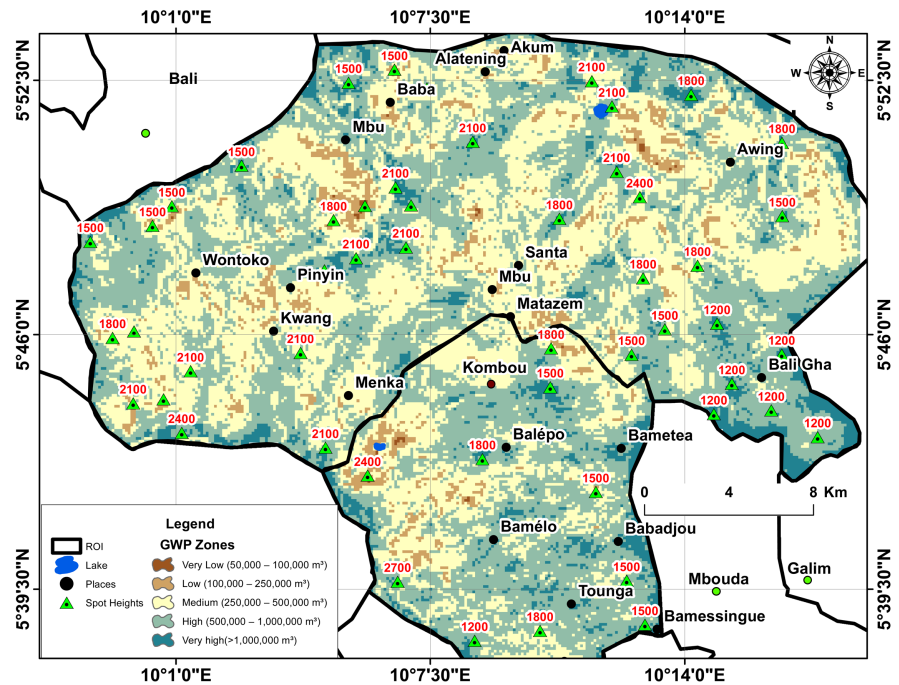
**Table 6.** Weights and ranks of the corresponding factors influencing groundwater potential zones.

Factor	Weight	Rank
Lithology	32.7	1
Slope	29.9	2
Relief and current surface water	17.9	3
Drainage density	10.4	4
Land use	6.8	5

Source: Derived from **Table 1**.

As illustrated in **Figure 9** and detailed out in **Table 7**, the spatial distribution of groundwater potential zones across the Santa-Babadjou Corridor reveals that a

dominant 95.11% of the total land area falls within the medium, high, and very high groundwater potential classes. Specifically, medium potential zones account for 40.69%, high zones cover the largest share at 46.02%, and very high zones make up 8.39% of the landscape.



Source: cumulatively derived from **Figures 3-8**.

**Figure 9.** Groundwater potential zones (GWPZ) of the Santa-Babadjou Corridor.

**Table 7.** Value, count, area and percentage of groundwater occurrence in the Santa-Babadjou Corridor.

Value	Count	Area (Ha)	Percentage (%)
Very low	44	115.4736	0.0977
Low	2161	5671.328	4.798384
Medium	18,324	48089.51	40.68745
High	20,727	54395.94	46.02318
Very high	3780	9920.232	8.393285

Source: Determined from **Figure 9**.

The results in **Figure 9** reveal that zones considered as favourable for groundwater potential are primarily found Babadjou, Alatening, and parts of Awing and Santa, where the lithology, slope, relief and current surface water sources, drainage density and land use factors enhance groundwater recharge. In contrast, 4.89% of the corridor falls under low (4.80%) and very low (0.10%) groundwater potential classes. These poorly rated zones are generally situated in the northwest-

ern and extreme highland parts of the corridor, which are characterized by steep slopes, rocky surfaces, high drainage density, and reduced permeability. The groundwater classification also corresponds to estimated potential volumes, ranging from very low zones ranging between 50,000 - 100,000 m<sup>3</sup>, low zones ranging between 100,000 - 250,000 m<sup>3</sup>, medium zones ranging from 250,000 - 500,000 m<sup>3</sup>, high zones between 500,000 - 1,000,000 m<sup>3</sup>, and very high zones with values exceeding 1,000,000 m<sup>3</sup>.

Areas with very good to good groundwater potential zones are typically found in regions with gentle slopes, permeable and porous lithologies (such as fractured basalts), low drainage density, high surface water availability, and favourable land cover types of forest, grassland, or cultivated land. These areas support higher infiltration and percolation into underground aquifers.

The six thematic layers integrated to generate the GWPZ map for the Santa-Babadjou Corridor exert varying degrees of influence on aquifer recharge and thus on the availability and spatial distribution of groundwater resources (**Figure 9**). The weightings derived through the Analytic Hierarchy Process approach yielded a Consistency Ratio (CR) of 1.84%, which is well below the acceptable threshold of 10%, indicating that the pairwise comparisons made in the AHP model are logically consistent. This affirms the reliability and robustness of the resulting GWPZ map. Similar findings in comparable hydrogeological contexts have also been reported by (Abate et al., 2022; Abd-Elmaboud et al., 2024; Abdelrahman et al., 2023; Abdullahi et al., 2023; Abdullateef et al., 2021).

Zones with poor groundwater potential are typically characterized by steep slopes, dense drainage networks, sparse or degraded vegetation cover, forest-dominated land use, and less permeable lithologies like granite. These areas, largely found in the northwestern and elevated portions of the corridor, show reduced recharge potential due to enhanced surface runoff and limited infiltration capacity.

Geological and topographic attributes emerge as central to groundwater distribution in the corridor in that the older, weathered lithologies common in parts of Babadjou enhance porosity and permeability due to long-term fracturing and deformation. These processes improve secondary porosity, allowing groundwater to infiltrate and be stored effectively. Favourable relief conditions also signify structural weaknesses that serve as conduits for subsurface water movement, further boosting groundwater recharge. Similar studies have been reported in other fractured basement terrains like (Adewumi et al., 2023; Adiat et al., 2024; Akeredolu et al., 2025; Alarifi et al., 2022).

Slope is inversely related to infiltration hence, flatter terrains, which dominate the eastern parts of the Santa-Babadjou Corridor, experience reduced runoff and prolonged surface water residence time, promoting better groundwater infiltration. Similarly, low drainage density often co-located with gentle slopes indicates reduced surface flow and greater potential for aquifer recharge. Therefore, regions with such attributes align with the medium to very high groundwater potential

categories, collectively covering over 86.68% of the entire corridor, as seen in **Table 7**. This is consistent with other studies where similar physical conditions led to higher groundwater potential classifications (Adesola, 2024; Adesola et al., 2025; Agogue Feujio et al., 2024; Ahmad et al., 2021).

While built-up areas have low recharge potential due to impervious surfaces, the high groundwater potential identified in some developed areas of the corridor indicates that underlying geological formations and slope characteristics override surface constraints. This reinforces the understanding that land use effects on groundwater recharge are strongly mediated by subsurface lithology and topographic context, rather than surface development alone an insight supported by several authors working on urban hydrology and groundwater dynamics (Anusha et al., 2022; Fildes et al., 2022; Hu & Li, 2024; Saikia et al., 2023; Suprapti et al., 2024; Zhou et al., 2024).

It is worth mentioning as limitation that, though this study provides robust groundwater potential mapping, three key limitations should be noted. First, the analysis used static datasets that cannot account for seasonal recharge variability, particularly important in this region with distinct wet/dry cycles. Second, climate change impacts on long-term precipitation patterns and recharge rates were not incorporated, potentially affecting the future validity of these groundwater potential zones. Third, the single-time land use snapshot doesn't capture ongoing land cover changes that may alter infiltration capacity. Future studies would benefit from integrating time-series climate data and dynamic land use models to address these temporal limitations.

#### 4. Conclusion

This study demonstrates the efficiency of RS, GIS, and field surveys to delineate GWPZs in the Santa-Babadjou Corridor, a region characterized by complex geological and hydrological dynamics. By synthesizing multiple thematic layers: lithology, slope, relief, drainage density, and land use, this study provides a comprehensive framework for assessing groundwater recharge potential, offering critical insights for sustainable water resource management in the face of growing scarcity and anthropogenic pressures.

The findings reveal that lithology is the most influential factor in groundwater potential, with a weight of 32.7%, underscoring the significance of geological formations in controlling infiltration and aquifer storage. Late Tectonic Granites and alluvial deposits emerged as the most favorable lithological units due to their fractured and porous nature, respectively, while less permeable formations like Biotite and Amphibole Gneisses exhibited limited recharge capacity. Slope, the second most critical factor (29.9%), further modulated groundwater dynamics, with gentle slopes ( $\leq 9^\circ$ ) promoting infiltration and steep slopes ( $\geq 19^\circ$ ) exacerbating runoff. The spatial distribution of these factors highlighted the corridor's heterogeneity, where low-lying southern regions exhibited higher recharge potential compared to the rugged northern highlands. Also, Relief (17.9%) and drainage density

(10.4%) played intermediary roles, with elevation variations and stream network density influencing water retention and subsurface flow. Areas with moderate relief and low drainage density, such as central Babadjou and Alatening, were identified as optimal for groundwater recharge. Land use (6.8%), though less influential, revealed the impact of human activities, with farmlands and grasslands enhancing infiltration, while built-up areas and forests reduced it due to impervious surfaces and rapid runoff, respectively. The AHP model, validated by a consistency ratio of 1.84%, effectively integrated these factors to classify the corridor into five GWPZs: very poor (0.10%), poor (4.80%), moderate (40.69%), good (46.02%), and very good (8.39%). These zones align with observed hydrogeological conditions, where high-to-very-high-potential areas correlate with gentle slopes, permeable lithologies, and favorable land cover. Field validation using static water levels and spring locations confirmed the model's accuracy, reinforcing its utility for practical applications like borehole siting and agricultural planning.

The results of this study not only address the immediate water scarcity challenges in the Santa-Babadjou Corridor but also contribute to broader discourse on sustainable groundwater management in volcanic terrains. The methodological framework combining geospatial analysis, multi-criteria decision-making, and field validation can be adapted to other regions with similar hydrogeological complexities. Future research could explore temporal dynamics of recharge, climate change impacts, and the integration of machine learning to refine predictive models.

### Conflicts of Interest

The authors declare no conflicts of interest regarding the publication of this paper.

### References

- Abate, S. G., Amare, G. Z., & Adal, A. M. (2022). Geospatial Analysis for the Identification and Mapping of Groundwater Potential Zones Using RS and GIS at Eastern Gojjam, Ethiopia. *Groundwater for Sustainable Development*, 19, Article ID: 100824. <https://doi.org/10.1016/j.gsd.2022.100824>
- Abdelkareem, M., Mansour, A. M., & Akawy, A. (2024). Securing Water for Arid Regions: Rainwater Harvesting and Sustainable Groundwater Management Using Remote Sensing and GIS Techniques. *Remote Sensing Applications: Society and Environment*, 36, Article ID: 101300. <https://doi.org/10.1016/j.rsase.2024.101300>
- Abd-Elmaboud, M. E., Saqr, A. M., El-Rawy, M., Al-Arifi, N., & Ezzeldin, R. (2024). Evaluation of Groundwater Potential Using ANN-Based Mountain Gazelle Optimization: A Framework to Achieve SDGs in East El Oweinat, Egypt. *Journal of Hydrology: Regional Studies*, 52, Article ID: 101703. <https://doi.org/10.1016/j.ejrh.2024.101703>
- Abdelouhed, F., Ahmed, A., Abdellah, A., Yassine, B., & Mohammed, I. (2021). Using GIS and Remote Sensing for the Mapping of Potential Groundwater Zones in Fractured Environments in the CHAOUIA-Morocco Area. *Remote Sensing Applications: Society and Environment*, 23, Article ID: 100571. <https://doi.org/10.1016/j.rsase.2021.100571>
- Abdelrahman, K., Hazaea, S. A., Hazaea, B. Y., Abioui, M., & Al-Awah, H. (2023). Groundwater Potentiality in Hard-Rock Terrain of Southern Saudi Arabia Using Electrical Re-

- sistivity Tomography Approach. *Journal of King Saud University—Science*, 35, Article ID: 102928. <https://doi.org/10.1016/j.jksus.2023.102928>
- Abdullahi, A., Jothimani, M., Getahun, E., Gunalan, J., & Abebe, A. (2023). Assessment of Potential Groundwater Zones in the Drought-Prone Harawa Catchment, Somali Region, Eastern Ethiopia Using Geospatial and AHP Techniques. *The Egyptian Journal of Remote Sensing and Space Sciences*, 26, 628-641. <https://doi.org/10.1016/j.ejrs.2023.07.005>
- Abdullateef, L., Tijani, M. N., Nuru, N. A., John, S., & Mustapha, A. (2021). Assessment of Groundwater Recharge Potential in a Typical Geological Transition Zone in Bauchi, Nigeria Using Remote Sensing/GIS and MCDA Approaches. *Heliyon*, 7, e06762. <https://doi.org/10.1016/j.heliyon.2021.e06762>
- Abijith, D., Saravanan, S., Singh, L., Jennifer, J. J., Saranya, T., & Parthasarathy, K. S. S. (2020). GIS-Based Multi-Criteria Analysis for Identification of Potential Groundwater Recharge Zones—A Case Study from Ponnaniyar Watershed, Tamil Nadu, India. *HydroResearch*, 3, 1-14. <https://doi.org/10.1016/j.hydres.2020.02.002>
- Achu, A. L., Thomas, J., & Reghunath, R. (2020). Multi-Criteria Decision Analysis for Delineation of Groundwater Potential Zones in a Tropical River Basin Using Remote Sensing, GIS and Analytical Hierarchy Process (AHP). *Groundwater for Sustainable Development*, 10, Article ID: 100365. <https://doi.org/10.1016/j.gsd.2020.100365>
- Adesola, G. O. (2024). Modeling of Groundwater Productivity in the Alfred Nzo District, South Africa, Using Relative Frequency Ratio and Shannon Entropy Models. *Journal of Hydrology: Regional Studies*, 54, Article ID: 101877. <https://doi.org/10.1016/j.ejrh.2024.101877>
- Adesola, G. O., Gwavava, O., Pharoe, B. K., Baiyegunhi, C., Thamaga, K. H., & Muavhi, N. (2025). Appraising the Accuracy of GIS-Based Bivariate Statistical Model for Groundwater Potential Mapping in South Africa. *Heliyon*, 11, e43411. <https://doi.org/10.1016/j.heliyon.2025.e43411>
- Adewumi, R., Agbasi, O., & Mayowa, A. (2023). Investigating Groundwater Potential in Northeastern Basement Complexes: A Pulka Case Study Using Geospatial and Geo-Electrical Techniques. *HydroResearch*, 6, 73-88. <https://doi.org/10.1016/j.hydres.2023.02.003>
- Adiat, K. A., Kolawole, A. O., Adeyemo, I. A., Akinlalu, A. A., & Afolabi, D. O. (2024). Assessment of Groundwater Resources from Geophysical and Remote Sensing Data in a Basement Complex Environment Using Fuzzy-Topsis Algorithm. *Results in Earth Sciences*, 2, Article ID: 100034. <https://doi.org/10.1016/j.rines.2024.100034>
- Agogue Feujio, D. H., Aretouyap, Z., Tchato, S. C., Ngog II Legrand, C., Djomdi, E., Nague Madadjeu, N. et al. (2024). Application of Analytical Hierarchy Process to Assess Groundwater Potential for a Sustainable Management in the Menoua Division. *Heliyon*, 10, e24310. <https://doi.org/10.1016/j.heliyon.2024.e24310>
- Ahmad, I., Dar, M. A., Fenta, A., Halefom, A., Nega, H., Andualem, T. G. et al. (2021). Spatial Configuration of Groundwater Potential Zones Using OLS Regression Method. *Journal of African Earth Sciences*, 177, Article ID: 104147. <https://doi.org/10.1016/j.jafrearsci.2021.104147>
- Ahmad, I., Dar, M. A., Teka, A. H., Teshome, M., Andualem, T. G., Teshome, A. et al. (2020). GIS and Fuzzy Logic Techniques-Based Demarcation of Groundwater Potential Zones: A Case Study from Jemma River Basin, Ethiopia. *Journal of African Earth Sciences*, 169, Article ID: 103860. <https://doi.org/10.1016/j.jafrearsci.2020.103860>
- Ahmadou, A., Ondo, A. D. B., Sini, A., & Nguetnkam, J. P. (2023). Morphological, Mineralogical and Geochemical Characterization of the Danfili-Mambal Duricrust Formations (Adamawa-Cameroon). *Scientific African*, 21, e01873.

<https://doi.org/10.1016/j.sciaf.2023.e01873>

Ahmed, S., Haque, K. E., Moniruzzaman, M., Suborna, M. A. K., Anonna, T. A., Quaiyum Bhuyian, M. A. et al. (2025). Hydrogeochemistry, Water Quality, and Potential Human Health Risk Assessment of Groundwater in a Drought-Prone Area, Bangladesh. *Groundwater for Sustainable Development*, 29, Article ID: 101450.

<https://doi.org/10.1016/j.gsd.2025.101450>

Aind, D. A., Dasgupta, S., & Mukherjee, A. (2025). Novel Finding of Occurrence of Geo-genic Nickel in the Arsenic-Enriched Groundwater of the Himalayan Brahmaputra River Basin Aquifers. *Journal of Hydrology*, 659, Article ID: 133249.

<https://doi.org/10.1016/j.jhydrol.2025.133249>

Akeredolu, B. E., Adiat, K. A. N., Olayanju, G. M., Akinlalu, A. A., & Afolabi, D. O. (2025). Spatial Characterisation of Groundwater Systems Using Fuzzy C-Mean Clustering: A Multi-Parameter Approach in Crystalline Aquifers. *Results in Earth Sciences*, 3, Article ID: 100051. <https://doi.org/10.1016/j.rines.2024.100051>

Akiang, F. B., Nnaji, V. N., Opara, A. I., Agoha, C. C., Agbasi, O. E., Ulem, E. B. et al. (2025). Geospatial and Geo-Electrical Assessment of Groundwater Vulnerability and Potential in Parts of Cross River, Southern Nigeria. *HydroResearch*, 8, 58-73.

<https://doi.org/10.1016/j.hydres.2024.09.007>

Aiao, J. O., & Abubakar, F. (2025). Groundwater Exploration, Management Strategies and Sustainability: Geophysical Approaches. *Geosystems and Geoenvironment*, 4, Article ID: 100395. <https://doi.org/10.1016/j.geogeo.2025.100395>

Alarifi, S. S., Abdelrahman, K., & Hazaea, B. Y. (2022). Depicting of Groundwater Potential in Hard Rocks of Southwestern Saudi Arabia Using the Vertical Electrical Sounding Approach. *Journal of King Saud University—Science*, 34, Article ID: 102221.

<https://doi.org/10.1016/j.jksus.2022.102221>

Alikhanov, B., Juliev, M., Alikhanova, S., & Mondal, I. (2021). Assessment of Influencing Factor Method for Delineation of Groundwater Potential Zones with Geospatial Techniques. Case Study of Bostanlik District, Uzbekistan. *Groundwater for Sustainable Development*, 12, Article ID: 100548. <https://doi.org/10.1016/j.gsd.2021.100548>

Anaba Fotze, Q. M., Bikoro Bi Alou, M., Djieto Lordon, A. E., Sep Nlomngan, J. P., Aboubakar, A., Blaise Haman, D. J. et al. (2025). Discrimination of Potential Groundwater Areas Using Remote Sensing, Gravity and Aeromagnetic Data in Rey Bouba and Environs, North Cameroon. *Groundwater for Sustainable Development*, 30, Article ID: 101455. <https://doi.org/10.1016/j.gsd.2025.101455>

Anaba Onana, A. B., Ndam Ngoupayou, J. R., & Mvondo Ondo, J. (2017). Analysis of Crystalline Bedrock Aquifer Productivity: Case of Central Region in Cameroon. *Groundwater for Sustainable Development*, 5, 66-74.

<https://doi.org/10.1016/j.gsd.2017.05.003>

Anusha, B. N., Pradeep Kumar, B., Rajasekhar, M., & Raghu Babu, K. (2022). Delineation of Groundwater Potential Zones Using Geospatial and MCDM Approaches in Urban Areas of Anantapur District, AP, India. *Urban Climate*, 46, Article ID: 101341.

<https://doi.org/10.1016/j.uclim.2022.101341>

Arauzo, M., García, G., & Valladolid, M. (2019). Assessment of the Risks of N-Loss to Groundwater from Data on N-Balance Surplus in Spanish Crops: An Empirical Basis to Identify Nitrate Vulnerable Zones. *Science of the Total Environment*, 696, Article ID: 133713. <https://doi.org/10.1016/j.scitotenv.2019.133713>

Aretouyap, Z., Billa, L., Jones, M., & Richter, G. (2020). Geospatial and Statistical Interpretation of Lineaments: Salinity Intrusion in the Kribi-Campo Coastland of Cameroon. *Advances in Space Research*, 66, 844-853. <https://doi.org/10.1016/j.asr.2020.05.002>

- Arshad, A., Zhang, Z., Zhang, W., & Dilawar, A. (2020). Mapping Favorable Groundwater Potential Recharge Zones Using a GIS-Based Analytical Hierarchical Process and Probability Frequency Ratio Model: A Case Study from an Agro-Urban Region of Pakistan. *Geoscience Frontiers*, *11*, 1805-1819. <https://doi.org/10.1016/j.gsf.2019.12.013>
- Arthur, E., Gyamfi, C., Kyekyeku Anyemedu, F. O., & Gyampo, M. (2025). SPATIAL and Temporal Dynamics of Groundwater Vulnerability to Contaminants under Climate and Land Use Changes in the Pra and Ankobra Basins. *Watershed Ecology and the Environment*, *7*, 208-229. <https://doi.org/10.1016/j.wsee.2025.05.001>
- Arunbose, S., Srinivas, Y., Rajkumar, S., Nair, N. C., & Kaliraj, S. (2021). Remote Sensing, GIS and AHP Techniques Based Investigation of Groundwater Potential Zones in the Karumeniyar River Basin, Tamil Nadu, Southern India. *Groundwater for Sustainable Development*, *14*, Article ID: 100586. <https://doi.org/10.1016/j.gsd.2021.100586>
- Ashagrie, W. A., Tarkegn, T. G., Ray, R. L., Tefera, G. W., Demessie, S. F., Tsegaye, L. et al. (2025). Assessing the Vulnerability of Groundwater to Pollution under Different Land Management Scenarios Using the Modified DRASTIC Model in Bahir Dar City, Ethiopia. *Heliyon*, *11*, e42660. <https://doi.org/10.1016/j.heliyon.2025.e42660>
- Aulenta, F., Tucci, M., Cruz Viggi, C., Milia, S., Hosseini, S., Farru, G. et al. (2025). Groundwater Electro-Bioremediation via Diffuse Electro-Conductive Zones: A Critical Review. *Environmental Science and Ecotechnology*, *23*, Article ID: 100516. <https://doi.org/10.1016/j.ese.2024.100516>
- Aumar, C., Labazuy, P., Buvat, S., & Delage, E. (2023). Self-Potential Dataset for Mapping Groundwater Flow Patterns in the Chaîne Des Puys (Auvergne, France). *Data in Brief*, *50*, Article ID: 109533. <https://doi.org/10.1016/j.dib.2023.109533>
- Ayikpa, K. J., Jofack Sokeng, V., Ballo, A. B., Gouton, P., & Kouamé, K. F. (2025). Multi-source Satellite Imagery and Machine Learning for Detecting Geological Formations in Cameroon's Western Highlands. *Signals*, *6*, Article No. 12. <https://doi.org/10.3390/signals6010012>
- Azinwi Tamfuh, P., Kouankap Nono, D. G., Wotchoko, P., Tchagnian Mbezele, B., Tene Djoukam, J. F., Kamgang Kabeyene, V. B. et al. (2020). Geochemistry of a Lateritic Mantle Developed on Basalt in the Cameroon Western Highlands (Cameroon Volcanic Line). *Geoderma*, *376*, Article ID: 114569. <https://doi.org/10.1016/j.geoderma.2020.114569>
- Banerjee, K., Santhosh Kumar, M. B., & Tilak, L. N. (2021). Delineation of Potential Groundwater Zones Using Analytical Hierarchy Process (AHP) for Gautham Buddh Nagar District, Uttar Pradesh, India. *Materials Today: Proceedings*, *44*, 4976-4983. <https://doi.org/10.1016/j.matpr.2020.12.917>
- Boas, T., & Mallants, D. (2022). Episodic Extreme Rainfall Events Drive Groundwater Recharge in Arid Zone Environments of Central Australia. *Journal of Hydrology: Regional Studies*, *40*, Article ID: 101005. <https://doi.org/10.1016/j.ejrh.2022.101005>
- Deka, D., Ravi, K., & Nair, A. M. (2025). Impact of Urbanisation on Groundwater Vulnerability in Shallow Aquifer System of Assam: A DRASTIC Approach. *Urban Climate*, *59*, Article ID: 102299. <https://doi.org/10.1016/j.uclim.2025.102299>
- Fildes, S. G., Bruce, D., Clark, I. F., Raimondo, T., Keane, R., & Batelaan, O. (2022). Integrating Spatially Explicit Sensitivity and Uncertainty Analysis in a Multi-Criteria Decision Analysis-Based Groundwater Potential Zone Model. *Journal of Hydrology*, *610*, Article ID: 127837. <https://doi.org/10.1016/j.jhydrol.2022.127837>
- Hu, J., & Li, X. (2024). Deformation Mechanism and Treatment Effect of Deeply Excavated Expansive Soil Slopes with High Groundwater Level: Case Study of MR-SNWTP, China. *Transportation Geotechnics*, *46*, Article ID: 101253. <https://doi.org/10.1016/j.trgeo.2024.101253>

- Ishola, K. S., Fatoyinbo, A. A., Hamid-Mosaku, A. I., Okolie, C. J., Daramola, O. E., & Lawal, T. O. (2023). Groundwater Potential Mapping in Hard Rock Terrain Using Remote Sensing, Geospatial and Aeromagnetic Data. *Geosystems and Geoenvironment*, 2, Article ID: 100107. <https://doi.org/10.1016/j.geogeo.2022.100107>
- Kaushik, P. R., Ndehedehe, C. E., Kalu, I., Burrows, R. M., Noll, M. R., & Kennard, M. J. (2023). Identifying Potential Hotspots of Groundwater-Climate Interaction in the Great Artesian Basin, Australia. *Ecological Informatics*, 78, Article ID: 102354. <https://doi.org/10.1016/j.ecoinf.2023.102354>
- Ma, L., Sun, X., Qian, J., Wang, W., Deng, Y., & Fang, Y. (2024). Identification of High-Permeability and Water-Rich Zones in a Fractured Karst Water Source Area Based on the Hydraulic Tomography Method. *Journal of Hydrology*, 629, Article ID: 130648. <https://doi.org/10.1016/j.jhydrol.2024.130648>
- Mahindawansa, A., & Gassmann, M. (2024). Spatio-Temporal and Depth-Oriented Evaluation of Hyporheic Zone Processes in Headwater Catchments. *Journal of Hydrology*, 645, Article ID: 132149. <https://doi.org/10.1016/j.jhydrol.2024.132149>
- Medhi, S., & Choudhury, R. (2025). Spatial and Temporal Distribution of Arsenic in Groundwater of the Brahmaputra River Floodplains in Assam, India. *Groundwater for Sustainable Development*, 28, Article ID: 101400. <https://doi.org/10.1016/j.gsd.2024.101400>
- Medrano-Pérez, O. R., Bustamante-Orozco, M. R., & Neri-Flores, I. (2023). Analysis of Aquifers Zones Using Aeromagnetic and Satellite Gravimetric Data in Grijalva and Usamacinta Basins, Mexico. *Groundwater for Sustainable Development*, 23, Article ID: 101001. <https://doi.org/10.1016/j.gsd.2023.101001>
- Mfonka, Z., Kouassy Kaledje, P. S., Anaba Onana, A., Nsangou, D., Kpoumie, A., Zammouri, M. et al. (2025). Integrated Geophysical and Remote Sensing/GIS Interpretation for Delineating the Structural Elements and Groundwater Aquifers of the Fouban Locality, Western Highlands of Cameroon (WHC). *Geosystems and Geoenvironment*, 4, Article ID: 100343. <https://doi.org/10.1016/j.geogeo.2024.100343>
- Mohammed, M. A. A., Szabó, N. P., Suliman, E. D., Siddig, M. M. S., Hassan, M. N. M., & Szűcs, P. (2025). Integrated Assessment of Human Health Risks from Groundwater Pollutants in Nubian Aquifer, Sudan: Combining Source Apportionment and Probabilistic Analysis. *Environmental Challenges*, 20, Article ID: 101176. <https://doi.org/10.1016/j.envc.2025.101176>
- Momo, M. N., Beauvais, A., Tematio, P., & Yemefack, M. (2020). Differentiated Neogene Bauxitization of Volcanic Rocks (Western Cameroon): Morpho-Geological Constraints on Chemical Erosion. *Catena*, 194, Article ID: 104685. <https://doi.org/10.1016/j.catena.2020.104685>
- Mosaad, S., Kotb, A. D. M., & Basheer, A. A. (2024). Groundwater Potentiality Mapping: A Case Study in Baba and Sidri Watersheds, South Sinai, Egypt. *Journal of African Earth Sciences*, 210, Article ID: 105145. <https://doi.org/10.1016/j.jafrearsci.2023.105145>
- Mu, D., Li, P., & De Baets, B. (2025). Biogeochemical Mechanisms and Biomarkers of Groundwater Salinization in Jinghuiqu Irrigation District, China. *Journal of Environmental Management*, 385, Article ID: 125631. <https://doi.org/10.1016/j.jenvman.2025.125631>
- Ngwese, S. N., Mouri, H., Akoachere, R. A. I., McKinley, J., & Candeias, C. (2025). Assessment of Potentially Harmful Elements in Surface and Groundwater from the Granitic Gneissic Aquiferous Formations in Bertoua City and Environs, East Region, Cameroon, Central Africa: Effects on Human Health. *Groundwater for Sustainable Development*, 29, Article ID: 101420. <https://doi.org/10.1016/j.gsd.2025.101420>
- Njumbe, L. J. N., Lordon, A. E. D., & Agyingi, C. M. (2023). Determination of Groundwater

Potential Zones on the Eastern Slope of Mount Cameroon Using Geospatial Techniques and Seismoelectric Method. *SN Applied Sciences*, 5, Article No. 238.

<https://doi.org/10.1007/s42452-023-05458-w>

Saaty, T. L. (1984). The Analytic Hierarchy Process: Decision Making in Complex Environments. In R. Avenhaus, & R. K. Huber (Eds.), *Quantitative Assessment in Arms Control: Mathematical Modeling and Simulation in the Analysis of Arms Control Problems* (pp. 285-308). Springer US. [https://doi.org/10.1007/978-1-4613-2805-6\\_12](https://doi.org/10.1007/978-1-4613-2805-6_12)

Saikia, P., Nath, B., & Dhar, R. K. (2023). Quantifying the Changing Pattern of Water Level Conditions and Groundwater Potential Zones in a Rapidly Urbanizing Kamrup Metropolitan District of Assam, India. *Groundwater for Sustainable Development*, 21, Article ID: 100935. <https://doi.org/10.1016/j.gsd.2023.100935>

Suprapti, S., Kusuma, M. S. B., Kardhana, H., & Cahyono, M. (2024). An Assessment of Potential Infiltration Areas to Support Groundwater Supply System in Jagakarsa, South Jakarta, Based on Multi-Criteria Decision-Making (MCDM) Analysis. *Case Studies in Chemical and Environmental Engineering*, 10, Article ID: 100799.

<https://doi.org/10.1016/j.cscee.2024.100799>

Yasmine, Z. T., Ghomsi, F. E. K., Nouayou, R., Pham, L. T., Aretouyap, Z., Kana, J. D. et al. (2024). Tectonic Reevaluation of West Cameroon Domain: Insights from High-Resolution Gravity Models and Advanced Edge Detection Methods. *Journal of Geodynamics*, 162, Article ID: 102061. <https://doi.org/10.1016/j.jog.2024.102061>

Zhou, Y., Zhang, Q., Bai, G., Zhao, H., Shuai, G., Cui, Y. et al. (2024). Groundwater Dynamics Clustering and Prediction Based on Grey Relational Analysis and LSTM Model: A Case Study in Beijing Plain, China. *Journal of Hydrology: Regional Studies*, 56, Article ID: 102011. <https://doi.org/10.1016/j.ejrh.2024.102011>